J Wood Sci (2000) 46:8–15

ORIGINAL ARTICLE

Yoshitaka Kubojima · Takeshi Okano · Masamitsu Ohta

Bending strength and toughness of heat-treated wood

Received: September 16, 1998 / Accepted: May 11, 1999

Abstract The load–deflection curve for static bending and the force–time curve for impact bending of heat-treated wood were examined in detail. The effect of oxygen in air was also investigated. Sitka spruce (*Picea sitchensis* Carr.) was heated for 0.5–16.0 h at a temperature of 160°C in nitrogen gas or air. The dynamic Young's modulus was measured by the free–free flexural vibration test, the static Young's modulus and work needed for rupture by the static bending test, and the absorbed energy in impact bending by the impact bending test. The results obtained were as follows: (1) The static Young's modulus increased at the initial stage of the heat treatment and decreased later. It decreased more in air than in nitrogen. (2) The bending strength increased at the initial stage of the heat treatment and decreased later. It decreased more in air than in nitrogen. (3) The work needed for rupture decreased steadily as the heating time increased. It decreased more in nitrogen than in air. It is thought that heat-treated wood was more brittle than untreated wood in the static bending test because W_{12} was reduced by the heat treatment. This means that the main factors contributing to the reduction of the work needed for rupture were viscosity and plasticity, not elasticity. (4) The absorbed energy in impact bending increased at the initial stage of the heat treatment and decreased later. It decreased more in air than in nitrogen. It was concluded that heat-treated wood became more brittle in the impact bending test because I_{12} and I_{23} were reduced by the heat treatment.

Y. Kubojima (✉)
Forestry and Forest Products Research Institute, Ministry of Agriculture, Forestry and Fisheries, PO Box 16, Tsukuba Norin Kenkyu Danchi-nai, Ibaraki 305-8687, Japan
Tel. +81-298-73-3211; Fax +81-298-73-3798
e-mail: kubojima@ffpri.affrc.go.jp

T. Okano[1] · M. Ohta
Graduate School of Agricultural and Life Sciences, The University of Tokyo, Tokyo 113-8657, Japan

Present address
[1]Wood Product Information Desk, Wood Information Hall, Woodyland Tokyo, Tokyo 135-0052, Japan

Key words Heat treatment · Impact bending · Toughness · Bending strength · Equilibrium moisture content

Introduction

In a previous paper[1] we examined the vibrational properties of sitka spruce heat-treated in nitrogen gas or in air. The density decreased at high temperature and with a long heating time. Generally, the specific Young's modulus, specific shear modulus, crystallinity index, and crystalline width increased at the initial stage of the heat treatment and decreased later. The loss tangent in the longitudinal (L)-direction increased under all conditions, whereas that in the radial (R)-direction decreased.

It has been said that wood becomes more brittle by heat treatment. The tensile strength of maple (*Acer* sp.) was increased by heat treatment at 400°F for 4.5 h.[2] The bending strength of hinoki wood (*Chamaecyparis obtusa* Endl.) heat-treated at 100°–150°C for 2–100 h became greater than that of untreated wood.[3] According to Kitahara and Chuganji,[4] the moduli of rupture in the bending of hinoki wood and buna wood (*Fagus crenata* Bl.) were not changed by 150°C treatment and were decreased to 50% that of untreated wood by 200°C treatment. The absorbed energy in impact bending was seriously decreased by the 150°C and 200°C treatments. Sato et al.[5] have reported that the fracture toughness decreases as the temperature exceeds 120°C.

We thought that the process of rupture during the bending test was related to the brittleness of the heat-treated wood. Hence, in this study the stress–strain curve during static bending and the force–time curve during impact bending were examined in detail. The curves were then divided into several parts, and we used the two-dimensional property (i.e., composed of the curve and the lateral axis) as the factor for the toughness of wood. The effect of oxygen in air was also investigated by heating wood in nitrogen gas or in air.

Experiment

Sitka spruce (*Picea sitchensis* Carr.) lumber, kiln-dried for piano soundboard, was used. It was stored in a room at 20°C and 65% relative humidity (RH) for more than a half-year and conditioned to a uniform moisture content. The specimens for the static bending test and the impact bending test were cut to the dimensions of 113 mm (L) × 7 mm (R) × 7 mm (T). Nine specimens were used for each heat treatment condition. Figure 1 shows the preparation of the specimens, and Table 1 shows their grouping.

After heat treatment and conditioning at 20°C and 65% RH for 2 weeks, the static bending and impact bending tests were conducted. The specimens were then immersed in water until the moisture content exceeded the fiber saturation point (average 113.1% and standard deviation 14.8% based on the oven-dried weight). They were then conditioned at 20°C and 65% RH again, and their weights, m_1, were measured. After measuring m_1, the oven-dried weights, m_0, were measured. The equilibrium moisture content at 20°C and 65% RH after the heat treatment, *EMC*, was obtained by the equation $EMC = 100(m_1 - m_0)/m_0$.

Table 1. Grouping of specimens

Group no.	Specimen no.[a]	Use
1	$10n + 1$	0.5 h Treatment
2	$10n + 2$	1 h Treatment
3	$10n + 3$	2 h Treatment
4	$10n + 4$	Control
5	$10n + 5$	4 h Treatment
6	$10n + 6$	8 h Treatment
7	$10n + 7$	16 h Treatment
8	$10n + 8$	Spare
9	$10n + 9$	Spare
10	$10n + 10$	Spare

[a] $n = 0, 1, 2, \ldots, 8$

Vibration test

To obtain the dynamic Young's modulus, a free–free flexural vibration test was conducted following the method described in our previous paper.[1] The dynamic Young's modulus was calculated by Euler-Bernoulli's equation.

Static bending test

The static bending test was performed using centerpoint loading over a 98-mm span with the load applied in the tangential direction. The cross-head speed was 4 mm/min. From the load-deflection (P-δ) curve the bending strength (σ), the static Young's modulus (E), and the work needed to deflect the specimens (W) were obtained.

The P-δ curve was divided into four parts as shown in Fig. 2. The four kinds of works W_{01}, W_{12}, W_{23}, and W_{34} were calculated as follows:

$$W_{01} = \int_0^{\delta_1} P d\delta \quad (1)$$

$$W_{12} = \int_{\delta_1}^{\delta_2} P d\delta \quad (2)$$

$$W_{23} = \int_{\delta_2}^{\delta_3} P d\delta \quad (3)$$

$$W_{34} = \int_{\delta_3}^{\delta_4} P d\delta \quad (4)$$

where P is the load, and δ is the deflection.

Impact bending test

Figure 3 shows the equipment used for the impact bending test. A Charpy-type impact bending machine with a capacity of 30 kgw·cm was used. The span was 84 mm. To obtain information on fracture mechanisms, an acceleration transducer with a capacity of $50g$ ($g = 9.81\,m/s^2$) was attached to

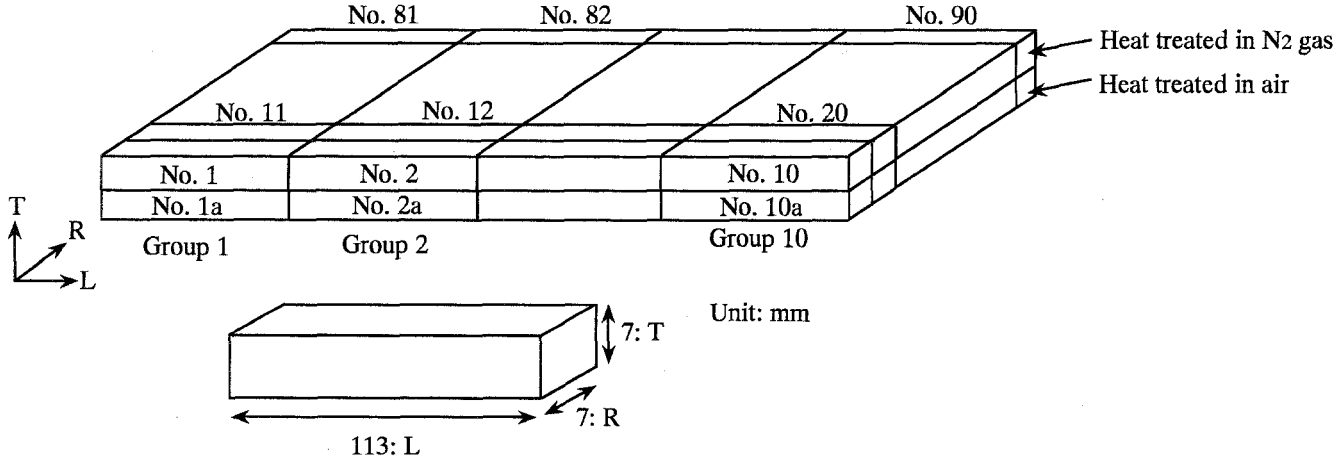

Fig. 1. Preparation of specimens

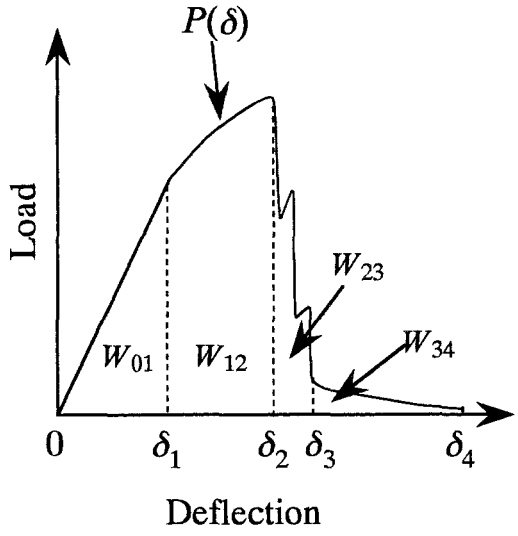

Fig. 2. Load–deflection curve

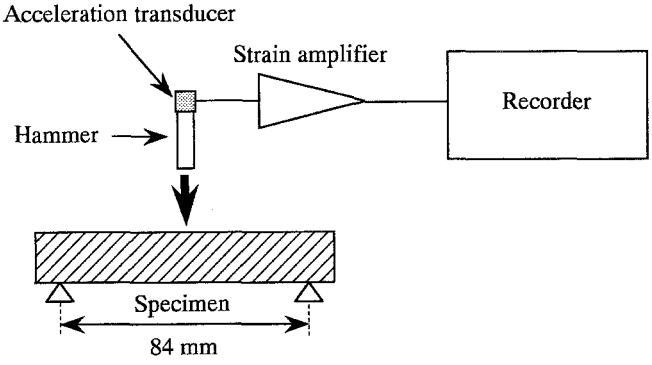

Fig. 3. Impact bending tester

the hammer of the machine. The output from the transducer was amplified and recorded;[6] then the force–time (F-t) curves were obtained (Fig. 4).

The absorbed energy in impact bending was obtained by the angle of the hammer when it was in the highest position (i.e., the potential energy of the hammer) and the F-t curve as follows.

The force for impact bending [$F(t)$] was obtained by the relation

$$F(t) = ma(t) \tag{5}$$

where t is the time, m (1.232 kg) is the mass of the hammer, and $a(t)$ is the acceleration.

Three kinds of impulses were obtained:

$$I_{01} = \int_0^{t_1} ma(t)dt \tag{6}$$

$$I_{12} = \int_{t_1}^{t_2} ma(t)dt \tag{7}$$

$$I_{23} = \int_{t_2}^{t_3} ma(t)dt \tag{8}$$

Fig. 4. Force–time curve

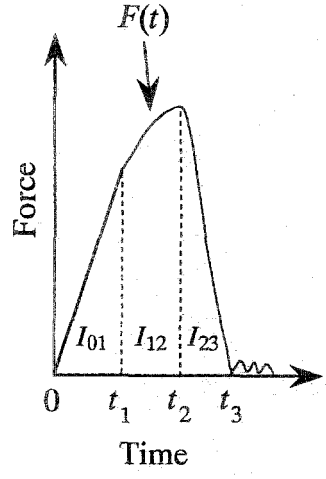

Then the absorbed energy in impact bending (W_{ib}) was calculated by:

$$W_{ib} = \frac{m}{2A}\left(v_0^2 - v^2\right)^2 \tag{9}$$

where A is the cross-sectional area, and h_0 is the initial height of the hammer.

$$v_0 = \sqrt{2gh_0}\,(= 2.15\,\text{m/s}) \tag{10}$$

$$v = \left(\frac{mv_0 - I_{03}}{m}\right)^2 \tag{11}$$

$$I_{03} = I_{01} + I_{12} + I_{23} \tag{12}$$

Heat treatment

For heat treatment, the equipment described in our previous paper[1] was used. The specimens were encapsulated in a pressure-resistant stainless steel portable reactor filled with nitrogen gas or air. The reactor was then heated in a constant-temperature oven at 160°C. The heating times were 0.5, 1, 2, 4, 8, and 16 h. The gases in the potable reactors were not refreshed during the heat treatment. After the heat treatment the specimens were left at 20°C and 65% RH for 2 weeks and then tested.

Results and discussion

Variation of properties in the test lumber

Because the effects of heat treatment on wood are not as drastic as those of chemical treatments,[7,8] it is necessary to take into consideration the variations of properties of the test lumber. Figures 5 and 6 show the variations in the density and the dynamic Young's modulus before the heat treatment, respectively. Note that the respective values slightly decrease with the increase in group number of the

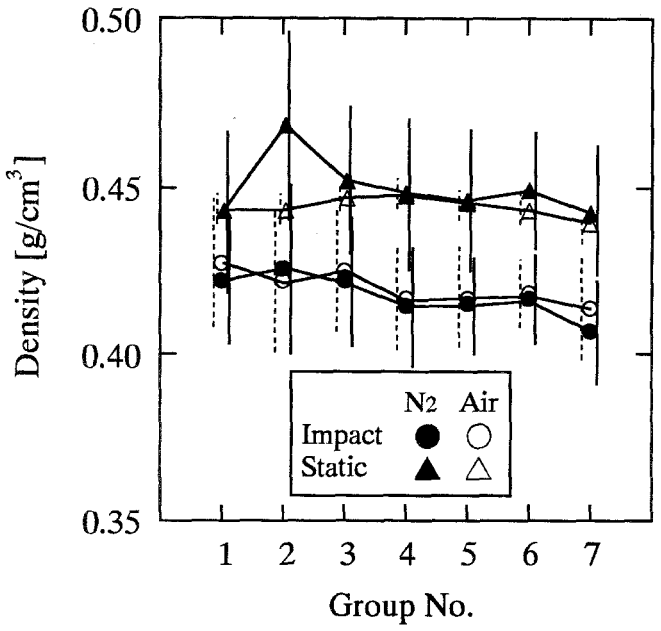

Fig. 5. Variation of density before heat treatment. Values are the average of each group. *Filled circles*, specimens heat-treated in N_2 gas for the impact bending test; *open circles*, specimens heat-treated in air for the impact bending test; *filled triangles*, specimens heat-treated in N_2 gas for the static bending test; *open triangles*, specimens heat-treated in air for the static bending test. *Solid lines at the right side of the filled symbols or dashed lines at the left side of the open symbols* are the standard deviation

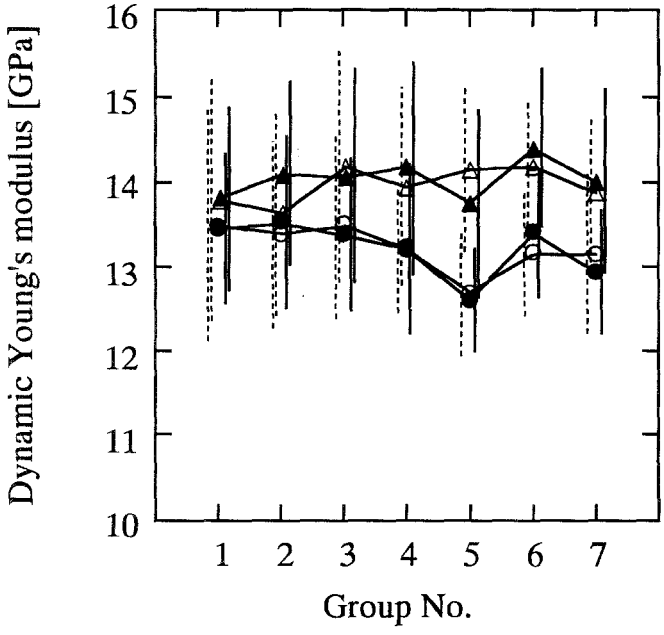

Fig. 6. Variation of dynamic Young's modulus before the heat treatment. Refer to Fig. 5 for explanation of symbols

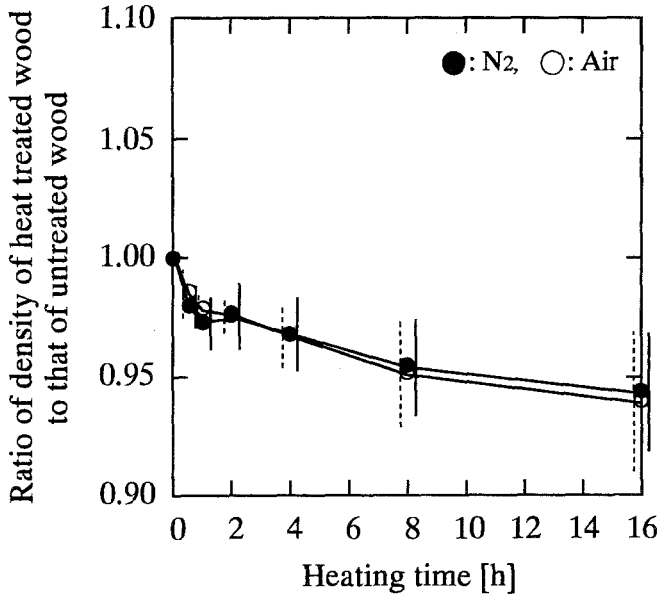

Fig. 7. Changes in density caused by heat treatment. The same specimens were used before and after treatment. *Filled circles*, specimens heat treated in N_2 gas; *open circles*, specimens heat treated in air. *Solid lines at the right side of the filled circles and dashed lines at the left side of the open circles* are the standard deviation

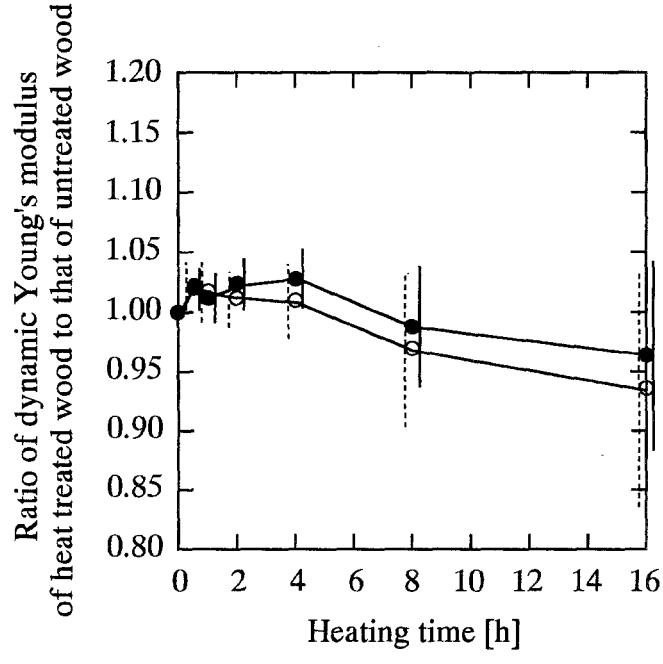

Fig. 8. Changes in dynamic Young's modulus caused by the heat treatment. Refer to Fig. 7 for explanation of symbols

specimens. Figures 7 and 8 show the changes in the density and the dynamic Young's modulus induced by the heat treatment, respectively. Here, the same specimen was used for the vibration test before and after the heat treatment. Hence, it was certain that the density decreased as the heating time increased, and that the dynamic Young's modulus increased at the initial stage of the heat treatment and decreased later. These tendencies were similar to those reported previously.[1,9] Therefore, it is thought that the decrease in values (e.g., the static Young's modulus, the work required to rupture, or the absorbed energy during impact bending) with the increase in heating time

(discussed later) were affected not only by the variations of the properties before the heat treatment but also by the heat treatment itself.

Change in equilibrium moisture content

Wood properties such as the Young's modulus, the bending strength, and the absorbed energy in impact bending depend on the moisture content of the specimens.[4,10,11] Figure 9 shows that the equilibrium moisture content decreased at 20°C and 65% RH after the heat treatment. This indicates that the fine structure of the specimens was changed. Hence, we used the Young's modulus, bending strength, and absorbed energy in impact bending without adjusting the moisture content.

Static bending test

Figure 10 shows the changes in the static Young's modulus caused by the heat treatment. The static Young's modulus increased at the initial stage of the heat treatment and was constant later in nitrogen, whereas in air it increased at the initial stage and decreased later. We think that the static Young's modulus will be decreased by heating longer, as for the dynamic Young's modulus in our previous paper[1] and Fig. 8. The static Young's modulus decreased more in air than in nitrogen gas.

Figure 11 shows the changes in bending strength caused by the heat treatment. The bending strength increased at the initial stage of the heat treatment and decreased later, as did the static Young's modulus. The bending strength decreased more in air than in nitrogen gas.

Figure 12 shows the changes in the work needed for rupture, $W_{04} = W_{01} + W_{12} + W_{23} + W_{34}$. The work for rupture decreased steadily with the heating time: It did not increase as did the static Young's modulus and the bending strength, at the initial stage of the heat treatment. The work for rupture decreased more in nitrogen gas than in air.

These results indicate that the wood was made more brittle by the heat treatment. It is thought that the tough-

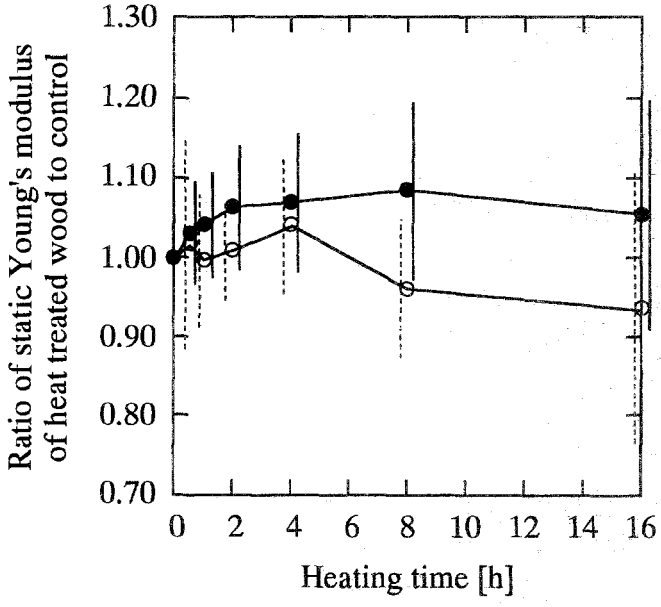

Fig. 10. Changes in static Young's modulus due to heat treatment. Values are the average of E/E_c in each group. E, static Young's modulus of heat-treated wood; E_c, static Young's modulus of control. Refer to Fig. 7 for explanation of symbols

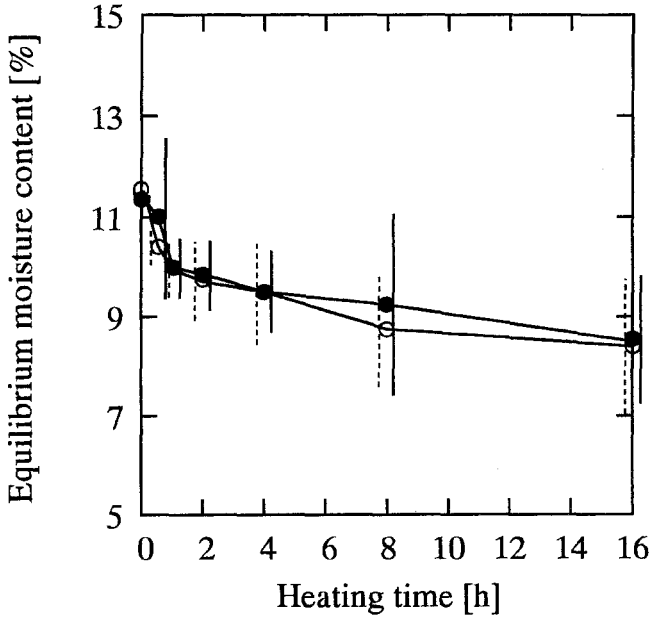

Fig. 9. Changes in equilibrium moisture content after heat treatment and immersion in water. Refer to Fig. 7 for explanation of symbols

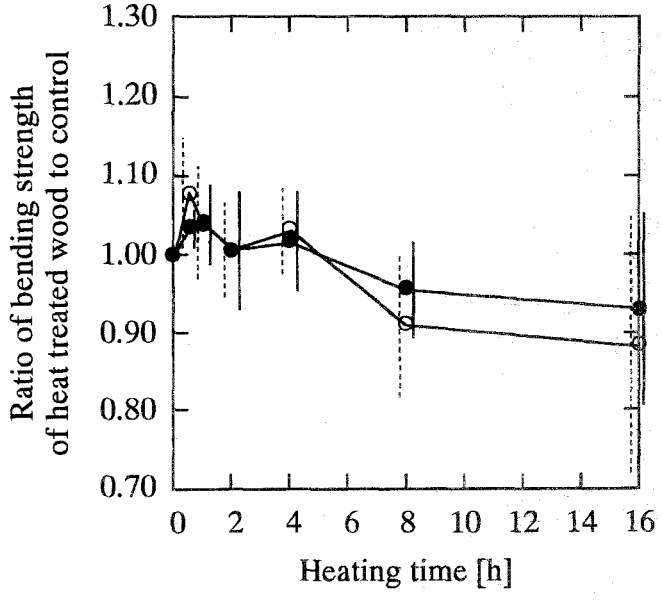

Fig. 11. Changes in bending strength due to heat treatment. Values are the average of σ/σ_c in each group. σ, bending strength of heat-treated wood; σ_c, bending strength of control. Refer to Fig. 7 for explanation of symbols

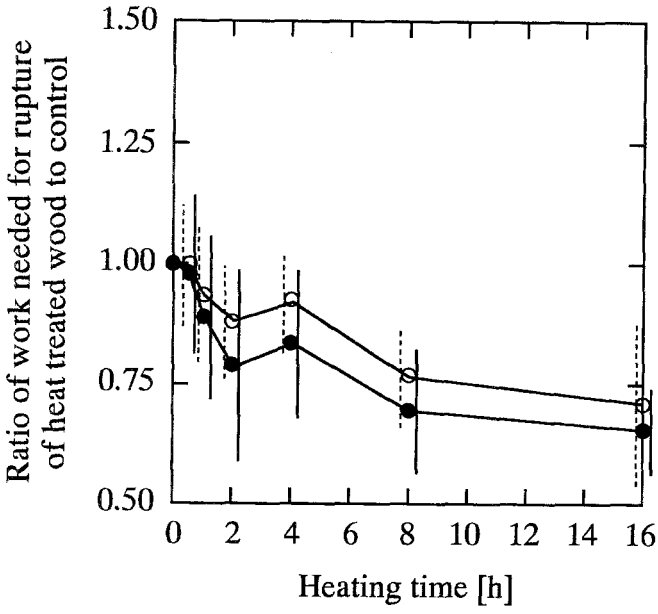

Fig. 12. Changes in work needed for rupture due to heat treatment. Values are the average of W_{04}/W_{04c} in each group. W_{04}, work needed for rupture of heat-treated wood; W_{04c}, work needed for rupture of control. Refer to Fig. 7 for explanation of symbols

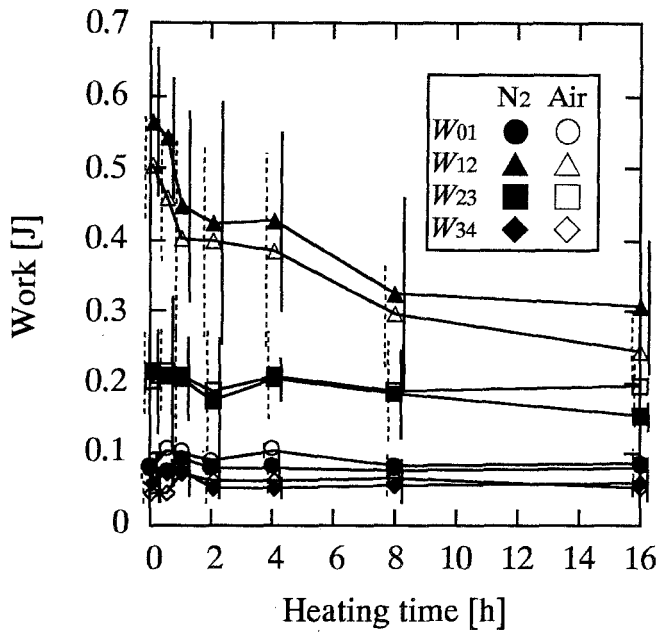

Fig. 13. Changes in work. Values are the average in each group. *Filled circles*, W_{01} of the specimens heat-treated in N_2 gas; *filled triangles*, W_{12} of the specimens heat-treated in N_2 gas; *filled squares*, W_{23} of the specimens heat-treated in N_2 gas; *filled diamonds*, W_{34} of the specimens heat-treated in N_2 gas; *open circles*, W_{01} of the specimens heat-treated in air; *open triangles*, W_{12} of the specimens heat-treated in air; *open squares*, W_{23} of the specimens heat-treated in air; *open diamonds*, W_{34} of the specimens heat-treated in air. *Solid lines at the right of the filled symbols and dashed lines at the left of the open symbols* are the standard deviation

ness of wood is related to its elasticity, viscosity, and plasticity. Thus, we investigated factors that possibly contribute to the change in W_{04} by dividing the force–deflection curve into four parts, as shown in Fig. 13.

Figure 13 shows the changes in each work part caused by the heat treatment. In this study, the boundary point between the linear region and the curve region, δ_1, could be fixed clearly. The values of W_{12} and W_{23} are larger than those of W_{01} and W_{34}. The change in W_{12} was largest and decreased as the heating time increased, whereas W_{34} did not change markedly. Hence, it was thought that heat-treated wood was more brittle in the static bending test than untreated wood because W_{12} was reduced by the heat treatment. Here, elasticity mainly affects W_{01}, which is the toughness of the linear region; other factors, such as viscosity or plasticity, affect W_{12}, W_{23}, and W_{34} which represent the toughness after the linear region. Therefore, we believe that the main factors contributing to the reduction of the work for rupture are viscosity and plasticity, rather than elasticity.

Impact bending test

Figure 14 shows the changes in the absorbed energy in impact bending obtained by the hammer's potential energy. The average of the ratio of W_{ib} obtained by the *F-t* curve to that by the hammer's potential energy was 0.91, with a standard deviation of 0.13. Based on these figures, the two values of W_{ib} were thought to be almost identical. It has been assumed that the value of W_{ib} derived from the hammer's potential energy is larger than that derived from the *F-t* curve because of the friction at the shaft of the hammer or the loss at the supporting point.[6]

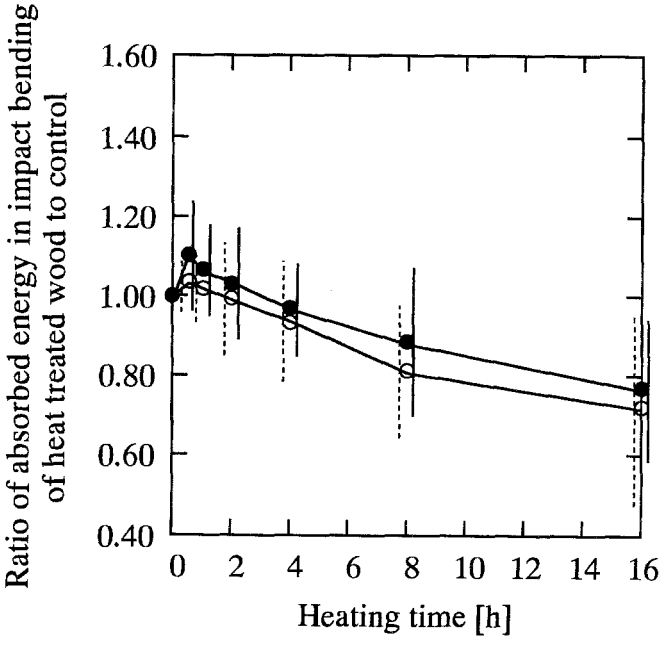

Fig. 14. Changes in absorbed energy in impact bending. Values are the average of the W_{ib}/W_{ibc} for each group, W_{ib}, absorbed energy in impact bending of heat-treated wood; W_{ibc}, absorbed energy in impact bending of control. Refer to Fig. 7 for explanation of symbols

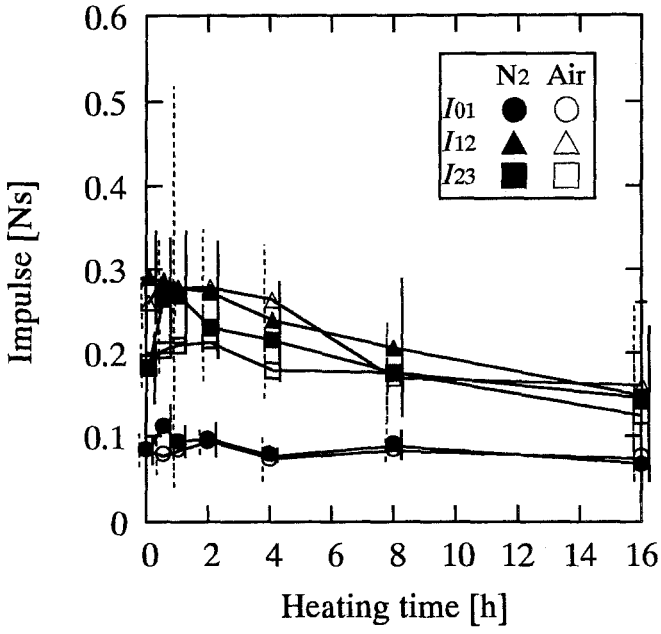

Fig. 15. Changes in impulse. *Filled circles*, I_{01} of the specimens heat-treated in N_2 gas; *filled triangles*, I_{12} of the specimens heat-treated in N_2 gas; *filled squares*, I_{23} of the specimens heat-treated in N_2 gas; *open circles*, I_{01} of the specimens heat-treated in air; *open triangles*, I_{12} of the specimens heat-treated in air; *open squares*, I_{23} of the specimens heat treated in air. *Solid lines at the right of the filled symbols or dashed lines at the left of the open symbols* are the standard deviation

The value of W_{ib} increased at the initial stage of the heat treatment and decreased later. This is different from W_{04} in the point of having a maximum value. We think that several aspects of this phenomenon (e.g., the loading speed and the relation of W_{04}-*EMC* and W_{ib}-*EMC*) should be investigated to clarify this difference. The absorbed energy in impact bending decreased more in air than in nitrogen gas.

Based on these results, it is thought that the wood was made more brittle by the heat treatment in impact bending as is the case with static bending. We believe that elasticity, viscosity, and plasticity are related to wood toughness, as for static bending, and so investigated the factors that contributed to the change in W_{ib} by dividing the force–time curve into three parts (Fig. 15).

Figure 15 shows the changes in each impulse part caused by the heat treatment. In this study the boundary point between the linear region and the curve region, t_1, could be fixed clearly, as for static bending. The values of and changes in I_{12} and I_{23} are larger than I_{01}; moreover, I_{12} and I_{23} decreased later in the heat treatment. Therefore, it is thought that the heat-treated wood became more brittle than untreated wood in terms of impact bending because I_{12} and I_{23} were reduced by the heat treatment.

Here, the stress–strain relation during impact bending is divided into a linear region and a nonlinear region.[6] If these regions of the force–time relation correspond to the respective regions of the stress–strain relation, it can be said that the main factors contributing to the reduction of absorbed energy in impact bending are viscosity and plasticity, rather than elasticity, as is the case with static bending.

Conclusions

The load–deflection curve for static bending and the force–time curve for impact bending of heat-treated wood were examined in detail. Sitka spruce (*Picea sitchensis* Carr.) wood was heated for 0.5 to 16 h at a temperature of 160°C in nitrogen or air. The results obtained are as follows.

1. The changes that occurred in the static Young's modulus, the work needed to rupture, and the absorbed energy during impact bending as the heating time increased were caused not only by the variation in the test lumber before the heat treatment but also by the heat treatment itself.
2. The static Young's modulus increased at the initial stage of the heat treatment and decreased later. It decreased more in air than in nitrogen.
3. The bending strength increased at the initial stage of the heat treatment and decreased later. It decreased more in air than in nitrogen.
4. The work needed for rupture decreased arithmetically with the heating time. It decreased more in nitrogen than in air. It is thought that the heat-treated wood was more brittle than untreated wood during the static bending test because W_{12} was reduced by the heat treatment. This means that the main factors contributing to the reduction of the work needed for rupture were viscosity and plasticity, not elasticity.
5. The absorbed energy during impact bending increased at the initial stage of the heat treatment and decreased later. It decreased more in air than in nitrogen. It was concluded that heat-treated wood became more brittle during the impact bending test because I_{12} and I_{23} were reduced by the heat treatment.

Acknowledgments We thank Mr. T. Yamada of Yamaha Company Ltd. for giving us the test lumber and Mr. T. Soma, a graduate student at The University of Tokyo, for his help in conducting our experiments.

References

1. Kubojima Y, Okano T, Ohta M (1998) Vibrational properties of sitka spruce heat treated in nitrogen gas. J Wood Sci 44:73–77
2. Clark GL, Howsmon JA (1946) Swollen, impregnated, and compressed wood samples. Ind Eng Chem 38:1257–1262
3. Hushitani M (1968) Effect of heat-treatment on static viscoelasticity of wood (in Japanese). Mokuzai Gakkaishi 14:208–213
4. Kitahara K, Chuganji M (1951) Effects of heat treatment on the mechanical properties of wood (in Japanese). J Jpn For Soc 33:414–419
5. Sato K, Yamamoto H, Kitani Y (1995) Influence of heat-treatment on fracture toughness and mechanical properties of wood (in Japanese). Bull Fac Educ Mie Univ 46:109–112
6. Ohta M, Asano I, Okano T (1979) Mechanical properties of brittleheart. II. Impact bending fracture (in Japanese). Mokuzai Gakkaishi 25:7–13
7. Yano H, Yamada T, Minato K, Komatsu K (1986) Changes in acoustical properties of sitka spruce due to reaction with formaldehyde (in Japanese). Mokuzai Gakkaishi 32:984–989
8. Yano H, Yamada T, Minato K (1986) Changes in acoustical properties of sitka spruce due to acetylation (in Japanese). Mokuzai Gakkaishi 32:990–995

9. Kajita S, Yamada T, Suzuki M (1961) Studies on rheological properties of wood. II. Effect of heat-treating condition on the hygroscopicity and dynamic Young's modulus of wood (in Japanese). Mokuzai Gakkaishi 7:34–38
10. Carrington H (1922) The elastic constants of spruce as influenced by moisture. Aeronaut J 26:462–471
11. Kollman FFP, Côté WA Jr (1968) Principles of wood science and technology. Springer, Berlin, pp 368–369